Diode laser overtone spectroscopy of atmospheric trace gases

Lucchesini A.,* Gozzini S.

Istituto di Fisica Atomica e Molecolare del CNR
Area della Ricerca di Pisa - Via Alfieri 1 (Loc. San Cataldo)
56010 Ghezzano S.G.T. (PI) - Italy

Abstract This work is based on the utilization of the diode lasers as spectroscopic sources for the observation and study of weak ro-vibrational overtone bands in the visible and near infrared spectra belonging to gases interesting from the environmental viewpoint. The diode lasers main characteristic is the possibility of the wavelength tuning on a resonance by properly driving their injection currents. This permits the direct observation of the absorption line-shapes. The resolution is limited by the lasers linewidth, generally ≈10–100 MHz. Also the excess laser amplitude $1/f$ noise can be reduced by using high frequency modulation techniques. It is shown that the diode lasers based spectroscopic apparata can extract very weak signals from the background with both good timing and spectral resolutions. The signal-to-noise ratio can be enhanced by using both the frequency modulation and phase sensitive techniques. Collisional broadening and shifting coefficients have been obtained by analyzing the line shapes of oxygen absorptions in the 760 nm electronic band, water vapor absorptions at around 820 nm, acetylene and ammonia absorptions in the 790 nm bands. Again, pressure broadening measurements have been carried on methane overtone resonances at around 860 nm. New lines have been observed by using the wavelength modulation spectroscopy technique with 2^{nd} harmonic detection. The sensitivity for each molecular species is shown in view of a possible practical application.

*E-mail: alex@ifam.pi.cnr.it

1 Introduction

Infrared laser spectroscopy gives unique possibilities for trace gas monitoring because of its high resolution, fast response and remote sensing capabilities. Nowadays single mode diode lasers (DLs) working at room temperature (RT) and emitting VIS and near IR radiation are commercially available at low cost. Most of them show good lasing characteristics and long operating lifetimes. The double heterostructure (DH) DLs then became the cheapest monochromatic sources in the field of the atomic and molecular spectroscopy. AlGaAs and InGaAlP DLs emissions can be easily tuned and scanned around most of the ro-vibrational overtone or electronic absorptions of molecules like CH_4, C_2H_2, C_2H_4, HCl, HCN, HF, H_2O, NH_3, NO_2, O_2, O_3, etc. with a good temporal resolution (≈10 ms). Methane [1], water vapor [2], acetylene [3], ammonia [4] overtones and oxygen weak lines belonging to the atmospheric A band have been observed in the past by conventional absorption spectroscopy in laboratory frames as well as in the earth atmosphere by using telescopes and the sun as light source [5]. Unfortunately these transition lines are usually weak and noise-reduction techniques must be used. Among them the frequency modulation (FM) technique [6] can be applied to DLs by directly modulating their injection current. When the frequency of the modulation is chosen much lower than the resonance line-width, the FM spectroscopy is usually called wavelength modulation (WM) spec-

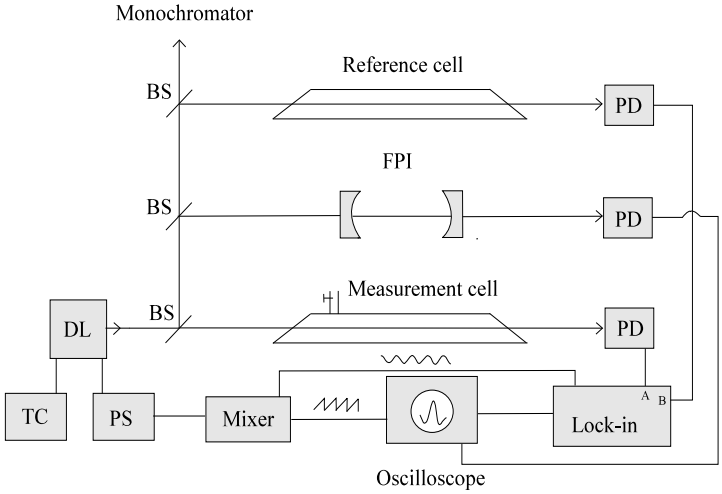

Figure 1: Outline of the experimental apparatus for the WM spectroscopy. DL: diode laser; BS: beam splitter; PD: photodiode; FPI: Fabry-Perot interferometer; TC: temperature controller; PS: power supply.

troscopy. The resolution of the DL spectroscopy technique is limited principally by the effective laser linewidth, which generally is ≈10–100 MHz in free running mode. Unfortunately a change in the injection current causes a variation of the emission power, inducing a typical sloping background on the transmitted signal, therefore, besides a FM, one has to deal with an amplitude modulation (AM). This brings to an asymmetry of the collected shapes that must be properly taken into account to avoid systematic errors in the data analysis.

2 Experimental apparata

Three different techniques and some different DLs have been used to detect and study the absorption features for overtone and combination vibrational transitions of O_2, H_2O, C_2H_2, CH_4, NH_3 gases. Direct absorption (DA) and wavelength modulation (WM) techniques have been adopted for the pressure broadening and shifting measurements, also the Two Tone Frequency Modulation (TTFM) technique has been used to detect some ammonia low absorptions.

An outline of the experimental apparatus adopted for the case of WM is shown in Fig. 1. The cw DLs here have single modes both transversely and longitudinally and their emission linewidths measure some tens of MHz. The observed absorption linewidths are always in the range of GHz (Doppler limited) at room temperature (RT), therefore the DL linewidth does not appreciably influence the measurements, provided we use a low modulation index [7]. The DL is driven by a stabilized low-noise current generator. A sinusoidal modulation at a frequency around 5–10 KHz is added to the DC current in the WM case. The signal at f or $2f$ is extracted by the aid of a lock-in amplifier. The latter case (second harmonic detection) is preferred, because the resulting second derivative of the absorption feature shows a nearly flat baseline, which is easier handled by the software, and gives greater resolution. The scan of the emission frequency is achieved by superimposing to the current signal the attenuated low frequency ($\sim$ 1 Hz) oscilloscope saw-tooth signal. The DL is temperature controlled within 0.002 °C through a Peltier junction powered by a temperature controller with a feedback system. The temperature dependence of the DLs emission wavelength is linear ($\sim$0.2 nm/°C), but with mode hops, and the current dependence for small current variations can be considered linear too ($\sim$0.01 nm/mA). The laser probe passes through a glass measurement cell a few times in order to reach a path of some meters. A beam splitter send 50% of the signal to a confocal FP interferometer to mark exactly the frequency sweep. A monochromator is employed for the rough wavelength reading. A silicon photodiode collects the signal, which is then sent to the lock-in amplifier and its output is shown on the oscilloscope. The analogic signal is collected and sampled by a data acquisition system driven by a desk-top computer. As known, the mode hops are the major DL drawback in free-running mode, which is the simplest and cheapest way of operation. This implies that in this configuration roughly only half of the covered spectrum can be really observed by a single DL. This obstacle can be overcome by using several DLs or by working in "extended cavity" [8] configuration. For the line-shift measurements the gas is hosted at a fixed pressure in the reference cell.

The electronic arrangement for the TTFM spectroscopy has been set up following the work of L. Wang and coworkers [9] with minor modifications. The complete set is displayed in Fig. 2. Still the emission frequency scan is obtained by using the oscilloscope saw-tooth properly attenuated. The microwave modulation signals are supplied by a 1 GHz Kruse Electronics radio frequency generator and the 10 MHz signal by a Wavetek Mod. 190 function generator. The Mini–Circuits ZFM 150 mixer produces a 1 GHz ± 10 MHz modulation signal, which is fil-

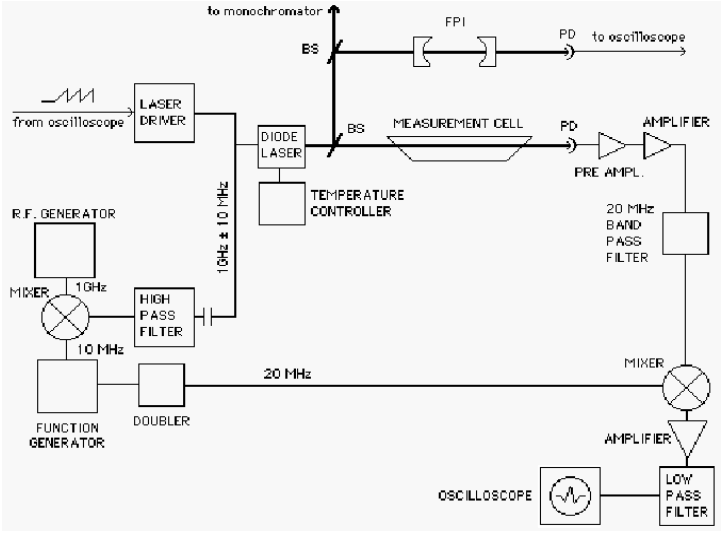

Figure 2: Sketch of the apparatus adopted for the TTFM spectroscopy. PD: photodiode; BS: beam splitter; FPI: Fabry-Perot interferometer.

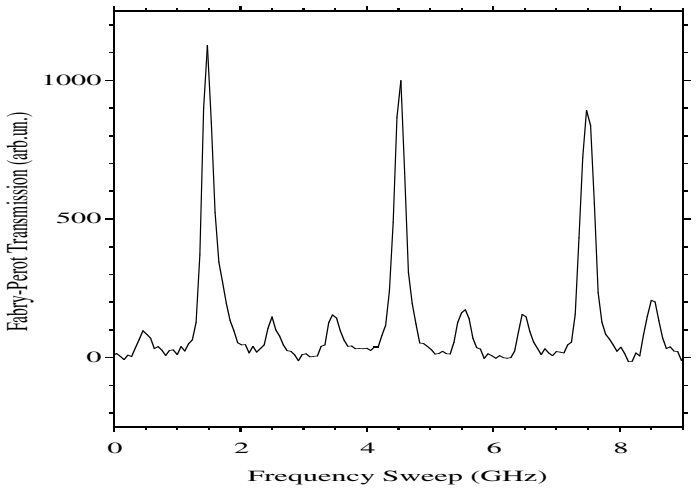

Figure 3: DL mode as seen through the Fabry-Perot interferometer when sweeping the DL emission frequency by 9 GHz. FSR = 3 GHz, Finesse $\simeq 12$.

tered by a K&L high-pass filter Mod. 3DH1; then the signal is capacitively coupled to the diode laser. The receiver is a EG&G FND 100 photodiode with its back connected to a FET preamplifier, whose exit signal is furtherly amplified by a QBit Mod. QB 9143 microwave amplifier. The signal is then filtered by a Mini–Circuits BPL 50 band-pass filter to permit only the 20 MHz beat signal to reach the ZFM 150 mixer. This receives also a 20 MHz signal coming from the function generator through a Mini–Circuits FK5 doubler. Only the *in-phase* signal is then sent to an oscilloscope through a 10 Hz low-pass filter. In Fig. 3 the transmission of the Fabry-Perot interferometer shows the Hitachi HL7801 DL emission mode with the side bands generated at 1 GHz. Here, as it always happens with DLs, the intensity varies with the frequency.

3 Line-shape analysis

A correct line shape analysis is important when studying the pressure broadening and shifting effects on the absorption features. In a previous work [14] a deep study has been carried on the line-shape collected by DL spectroscopy and specifically for the line-shift measurements.

When the harmonic detection is involved, the emission frequency $\bar{\nu}$ of the DLs is modulated sinusoidally by varying their injection current, the frequency being:

$$\nu = \bar{\nu} + m\cos\Omega t\,, \qquad (1)$$

where $\Omega = 2\pi\nu_m$, ν_m and m are respectively the frequency and the amplitude of the modulation. If $\bar{\nu}$ is slowly scanned over an interval across the chosen resonance, one gets a signal that depends on both the line shape and the modulation parameters. As an even function of the time, it can be written in a cosine Fourier series:

$$I(\bar{\nu} + m\,\cos\Omega t) = \sum_{n=0}^{\infty} H_n(\bar{\nu}, m)\,\cos n\Omega t\,, \qquad (2)$$

where $H_n(\bar{\nu})$ is the n-th harmonic component of the modulated signal. By demodulating the signal with a lock-in amplifier at a multiple $n\nu_m$ $(n = 1, 2, ...)$ of the modulation frequency, a signal proportional to the n-th component $H_n(\bar{\nu})$ is collected. If the amplitude m is smaller than the width of the transition line $(m \ll \gamma)$, the n-th Fourier component is proportional to the n-order derivative of the original signal:

$$H_n(\bar{\nu}, m) = \frac{2^{1-n}}{n!}\, m^n\, \left.\frac{d^n I(\nu)}{d\nu^n}\right|_{\nu=\bar{\nu}}, \qquad n \geq 1\,. \qquad (3)$$

3.1 Derivative spectroscopy limits

In general the intensity of a radiation $I(\nu)$ transmitted through an absorbing medium, $I(\nu) = I_0(\nu)\,T(\nu)$, can be described by the Lambert-Beer equation:

$$T(\nu) = e^{-\alpha(\nu)\,d}\,, \qquad (4)$$

where $T(\nu)$ is the transmittance, $d = \rho\,l$ is the optical density of the sample, which is the product of

the gas density ρ and the optical path l of the radiation through the sample, $\alpha(\nu)$ is the absorption coefficient. In case of weak absorptions $[\alpha(\nu)\, d \ll 1]$, that is always verified in our cases, Eq. (4) can be approximated by:

$$T(\nu) \simeq 1 - \alpha(\nu)\, d\,. \tag{5}$$

The $\alpha(\nu)$ coefficient must take into account the contribution of the Doppler broadening and the collisional (pressure) broadening. The Voigt function is the one that well describes it by the convolution of the Lorentz and the Gauss curves:

$$f(\nu) = \int_{-\infty}^{+\infty} \frac{\exp\left[-(t-\nu_\circ)^2/\Gamma_G^2 \ln 2\right]}{(t-\nu)^2 + \Gamma_L^2} dt\,, \tag{6}$$

where $\nu_\circ$ is the gas resonance frequency, Γ_G and Γ_L are the Gaussian and Lorentzian full width at half the maximum (FWHM) respectively. By revealing on the 2^{nd} harmonic one has to deal with the 2^{nd} derivative of the transmitted signal, therefore by assuming that the laser emission intensity varies linearly with the frequency, i.e. the injection current, (for DLs this is true for frequency sweeping up to a few tens of GHz, that is a few tens of mA):

$$I_0 = \bar{I}_0\,(1 + s\,\nu)\,, \tag{7}$$

where $\bar{I}_0$ is the intensity at $\nu = 0$ and s is the fractional variation per frequency unit. Then the second derivative of the transmitted power will be:

$$I''(\nu) = \bar{I}_0(1 + s\,\nu)\, T'' + 2\, s\, \bar{I}_0\, T'\,, \tag{8}$$

where $T'(\nu)$ and $T''(\nu)$ are the first and the second derivatives of the transmittance function. In the followings, in order to extract the line shape parameters, we used Eq. (8) and the fitting program LINEFIT [15].

3.2 Line-shift analysis

Fig. 4 displays the shapes of the signals corresponding to an absorption line and its second derivative in presence of a linear varying emission profile. As can be seen, the 2^{nd} derivative signal is not symmetric and the center of the line displaces from the maximum. The apparent shifting of the center depends on the slope s of the profile and on the width γ of the resonance line. This characteristic is very important when the pressure induced shift must be measured. By increasing the gas pressure, the width becomes

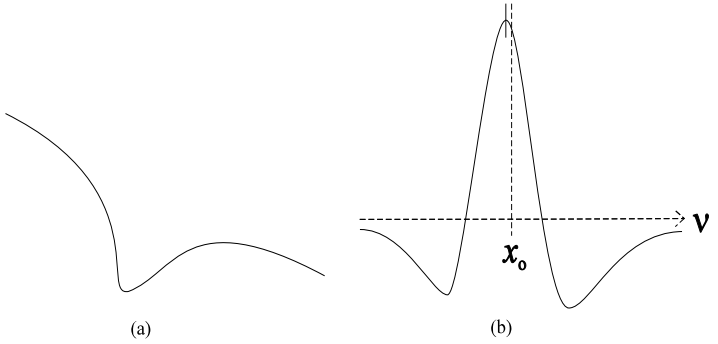

Figure 4: Direct absorption (left) and second derivative of the absorption (right) in presence of a non constant DL emission profile.

larger and a systematic shifting of the center occurs. This is proportional to the pressure in a way very similar to the *real* pressure induced shift.
For the sake of simplicity let us assume for the absorption coefficient $\alpha(\nu)$, a Lorentzian shaped function centered at $\nu = 0$, with a half width (HWHM) γ_L,

$$\alpha(\nu) = S\frac{\gamma_L}{\pi}\ \frac{1}{\nu^2 + \gamma_L^2}\,, \tag{9}$$

where S is the line strength. In the weak absorption approximation, that is Eq. (5), the transmittance is:

$$T(\nu) = 1 - S\, d\, \frac{\gamma_L}{\pi}\ \frac{1}{\nu^2 + \gamma_L^2}\,. \tag{10}$$

To get the shift of the maximum of the $2f$ signal, we expand the second derivative of Eq. (10) around $\nu = 0$:

$$\nu_{\max} = \frac{1}{4}\,\gamma_L \left(\xi - \frac{5}{16}\xi^3 + \cdots\right)\,, \tag{11}$$

where $\xi = s\,\gamma_L$ is the fractional variation of the intensity of the background relative to its value $I(0)$, at a distance γ_L from the center of the line.

For a numerical estimate we can reasonably assume $\xi = 0.1$, and calculate the displacement of the maximum as a function of the HWHM:

$$\frac{\nu_{\max}}{\gamma_L} = \frac{1}{4}\,\xi \simeq 0.025\,. \tag{12}$$

The displacement of about 2.5% of the width could be of the same order of magnitude of the pressure induced shift. Thus, if the maximum of the second derivative signal is used to determine the center of the line, the measurement of the pressure induced shift will result overestimated. A much more reliable measurement of the line-shape parameters is obtained by making a fit of the second derivative signal. Nevertheless, in the fit procedure one can be inclined to use

simply the 2^{nd} derivative of the absorption function, T'', and to multiply it by a sloping linear function to match the asymmetry of the experimental signal — this is equivalent to consider only the first term on the right side of Eq. (8). Although at a first sight the result of the fit could seem qualitatively satisfactory, the produced parameters are incorrect: the position of the center of the line will be again strongly affected by the pseudo-shift. The only correct choice for the fitting function is Eq. (8) that implicitly takes into account the presence of a non constant background. The slope of the background can be well determined by the direct absorption signal.

In the case of the pressure broadening effect, which is ten times larger than the shifting one, the choice of only the first term of Eq. (8) does not induce a significative error in the fit.

4 Experimental results

In the followings we will deal with substantially one kind of DL source: the DH AlGaAs Fabry-Perot type DL, emitting in the VIS and NIR [10]. Let us start showing the results obtained by using them.

4.1 Oxygen

The Sharp LT030MD DL has an emission wavelength around 755 nm at 25°C, therefore it must be warmed up to 45°C in order to reach the oxygen absorption lines of the $b^1\Sigma_g^+(\nu'=0) \leftarrow X^3\Sigma_g^-(\nu''=0)$ electronic transition band located at 760 nm. These are weak as they are forbidden by the electric dipole transition selection rules.

A small portion of the oxygen molecular spectrum is visible in Fig. 5, where the second derivatives of the ^{R}R(21) (13160.33 cm^{-1}, 759.655 nm @ 21°C), ^{R}R(19) (13160.81 cm^{-1}, 759.627 nm) and ^{R}R(23) (13161.60 cm^{-1}, 759.581 nm) oxygen absorption lines are shown. The line assignments come from the work of Babcock & Herzberg [5]; the wavelengths in air at 21°C have been deduced by using the index of refraction formula coming from the work of Edlén [11]. In the figure the asymmetry in the 2^{nd} derivative shapes is evident. Also the good S/N ratio is remarkable. As an example of the resolving power of the DL spectrometer in Fig. 6 two close weak lines are well distinguished to obtain for the peak distance: $\Delta\nu' = (6.4 \pm 0.1)$ cm^{-1}, in agreement to $\Delta\nu' = 6.3$ cm^{-1} obtained from HITRAN molecular database [12].

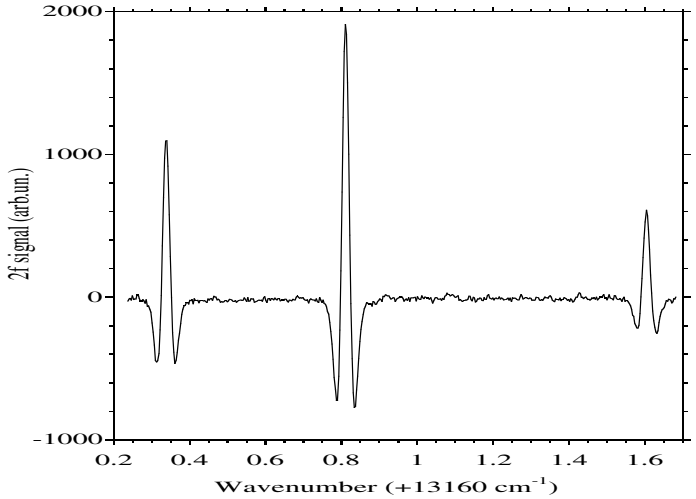

Figure 5: Second derivative of the oxygen absorption spectrum around 759.6 nm at 20 Torr and RT, through a 3 m absorption path (10 Hz bandwidth). The ^{R}R(21), the ^{R}Q(19) and the ^{R}R(23) lines are visible from left to right.

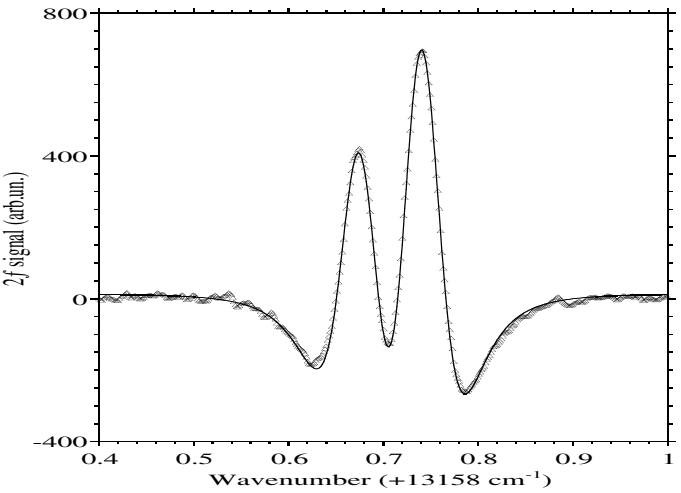

Figure 6: Two close weak oxygen absorption lines at 13158.67 cm^{-1} ^{R}R(19), and 13158.74 cm^{-1} ^{R}R(17) at atmospheric pressure and RT in a path-length of 3 m (triangles), along with the best fit (solid line). The lock-in time constant (τ) was 4 ms, corresponding to 30 Hz bandwidth.

Pressure broadening and shift in nitrogen (γ_{N_2}, S_{N_2}), and the self-broadening and self-shifting (γ_0, S_0) coefficients have been measured at RT for the more intense oxygen lines [13]. The average of the results are shown in Table 1. The results show that the shift effect is about an order of magnitude smaller than the broadening, but it is still well observed (here

Table 1: Averaged results of the oxygen FWHM line broadening (γ) and shifting (S) coefficients.

$\gamma_0 = 3.2$ MHz/Torr	$S_0 = -0.3$ MHz/Torr
$\gamma_{N_2} = 3.2$ MHz/Torr	$S_{N_2} = -0.3$ MHz/Torr

the error is on the first significant digit).
Also the work of Phillips & Hamilton [16] deals with the pressure shifting measurements of the same atmospheric oxygen band. Also their measurements always give negative shift coefficients, but theirs are about as double as ours.

A trend of the coefficients with the rotational quantum number N has been observed in the experimental data: the smaller is N, the smaller is the shift, and on the contrary the smaller is N, the higher is the broadening. Moreover, the results often show larger coefficients for N_2- than for self-broadening and shift.

A work on the oxygen A band has been carried out by Ritter & Wilkerson [17] by using a tunable dye laser along with a multipass White cell to reach a path length of 80 m. They got a list of self- and air-broadening coefficients. Some agreement with our results appears for the self-broadening of the ^{R}Q(7), ^{R}R(11) and ^{R}R(13) lines. For other lines there is a difference up to 30%. The main origin of this difference is presumably coming from the pressure narrowing (Dicke effect) they took into account to explain a deviation from the Voigt line shape observed in their measurements. Indeed we did not observe any appreciable deviation from the standard convolution of Gaussian and Lorentzian line shape in the pressure range 40–400 Torr. Ray & Ghosh [18, 19] measured the pressure broadening coefficients in our same spectral range by considering a Dicke narrowing too. Again their results are larger than ours. In any case our measurements are affected by a bigger error ought to the smaller optical path-length. Also Brown & Plymate [20] made a systematic work on the same band and their results on broadening and shifting are quite similar to ours, even if affected by a smaller error. They used the sophisticated Kitt Peak National Solar Observatory Fourier transform spectrometer (FTS) over approximately 12 m optical path length. Yang and coworkers [21] did an excellent work on pressure broadening by intracavity laser absorption spectroscopy (ICLAS), but in a wavelength range different from ours. Their results are comparable to the Brown's ones. Self- and N_2-broadening coefficients in the A band as function of the temperature have been obtained by Corsi and colleagues [22] still by using DL spectroscopy.

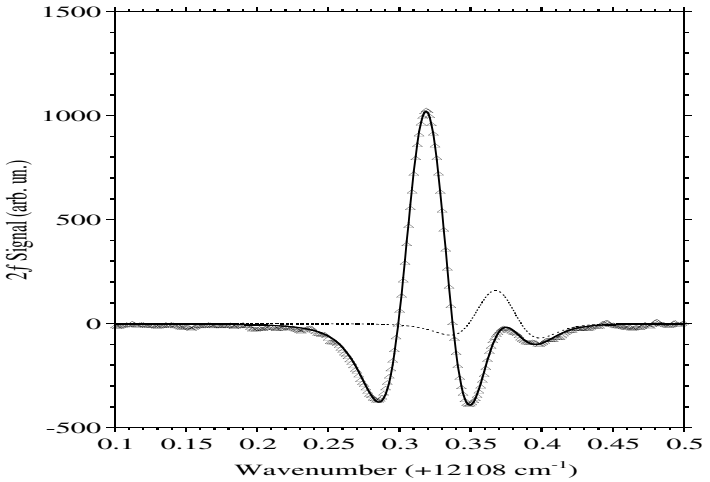

Figure 7: $2f$ signal of two water absorptions lines ($\triangle$) at 20 Torr, RT, 5 m absorption path, $\tau = 12.5$ ms (10 Hz bandwidth), along with the best fit.

By choosing the more intense observed oxygen absorption lines a sensitivity of some tens of ppm per meter of path length in open air has been obtained with our DL spectrometer. This system could be well applied in the high Tc superconductors production process where a fast and selective oxygen atmosphere monitoring in the chamber is required [23].

4.2 Water vapor

Even if working in free-running mode, the resolving power of the DL spectrometer is about 10^7; this and the high sensitivity permit to observe weak lines as shown in Fig. 7. They belong to the combination vibrational transition $(2,1,1) \leftarrow (0,0,0)$ and to the rotational transitions $1_{11} \leftarrow 2_{12}$ (12108.319 cm^{-1}), $5_{24} \leftarrow 5_{23}$ (12108.368 cm^{-1}). The S/N ratio is remarkable (~ 100).

For water vapor the adopted DL is the Hitachi HL8311G that has single longitudinal and transverse mode. It emits 15 mW coherent radiation at 830 nm. The observed absorption lines belong to the rovibrational overtone band $(2,1,1) \leftarrow (0,0,0)$, the strongest, $(3,1,0) \leftarrow (0,0,0)$, $(1,3,1) \leftarrow (0,0,0)$ band, as well as $(1,1,2) \leftarrow (0,0,0)$ band, the weakest. The measurement and reference cells were evacuated down to some tens of mTorr by a rotary pump, then a small quantity of distilled water has been let in and an equilibrium vapor pressure has been settled. After this operation the reference cell has been

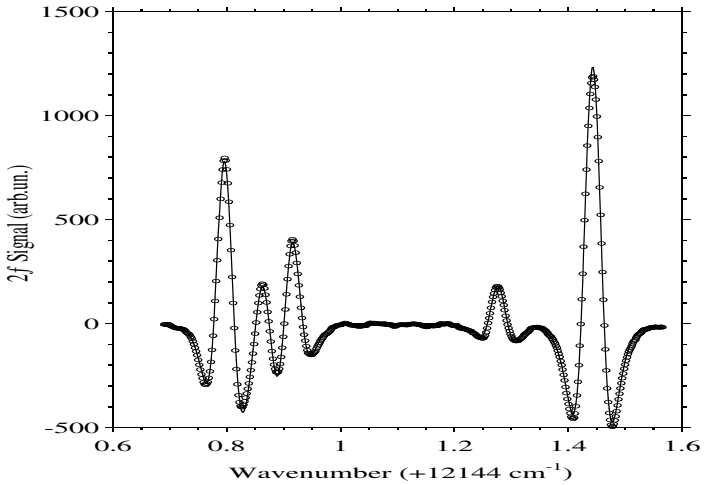

Figure 8: Water vapor spectrum around 12145 cm^{-1} with its best fit. The positions of the lines agree with what reported by HITRAN database: 12144.795, 12144.862, 12144.915, 12145.279, 12145.444 cm^{-1}, respectively. The H_2O pressure was its vapor pressure at RT, that is ~ 20 Torr. $\tau = 12.5$ ms.

sealed in order to maintain this equilibrium condition. Once an absorption line is found to be intense and well isolated from the others, the foreign gas was admitted in the measurement cell with a progression of some tens of Torr per time from about 20 to 400 Torr. An experiment lasted from 20 to 30 minutes and during this time the maximum drop caused by wall adsorption has been measured to be 2 Torr. This is compatible with what observed by others in different measurement cells [24]. In Fig. 8 a portion of the spectrum analyzed in this work in shown. The second derivatives of five water vapor lines are visible in a range spanning 1 cm^{-1} without any laser mode hop. According to HITRAN database all the lines belong to the $(2,1,1) \leftarrow (0,0,0)$ transition. Their positions agree with the ones listed by the database within 0.01 cm^{-1}. Here again the S/N is remarkable.

Broadening and shifting coefficient have been measured by the WM technique for the (2,1,1) band [25]. The average of the results for air-, H_2- and He-broadening and shifting are listed in Table 2. HITRAN database for the same lines gives an average of $\gamma_{\rm air}^{HITRAN} = 7.4$ MHz/Torr, that is little higher than ours.

The sensitivity of this diode laser spectroscope when locked on one of the more intense lines showed the possibility of detecting water vapor in the order of some tens of ppm per meter of optical path length.

Table 2: Averaged results of the observed water vapor FWHM broadening (γ) and shifting (S) coefficients.

$\gamma_{\rm air} = 6.9$ MHz/Torr	$S_{\rm air} = -0.5$ MHz/Torr
$\gamma_{\rm H_2} = 6.1$ MHz/Torr	$S_{\rm H_2} = -0.7$ MHz/Torr
$\gamma_{\rm He} = 1.9$ MHz/Torr	$S_{\rm He} = 0.1$ MHz/Torr

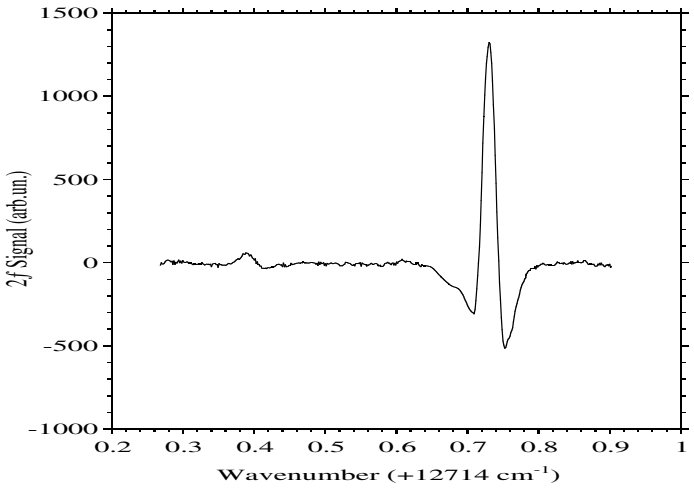

Figure 9: Acetylene absorption lines detected by WM spectroscopy at 38 Torr, $\tau = 12.5$ ms. The more intense of them lies at 12714.73 cm^{-1} ($\nu_1 + 3\nu_3$, R21). The other, whose origin is suggested in the text, is at (12714.39 ± 0.01) cm^{-1}.

4.3 Acetylene

In the case of the C_2H_2 spectroscopy two types of cw diode lasers have been utilized: the SHARP mod. LT024MDO for the $\nu_1 + 3\nu_3$ and $\nu_2 + 3\nu_3 + 2\nu_4$ combination overtone bands (790 nm), the STC mod. LT50A-03U for the $2\nu_1 + \nu_2 + \nu_3$ band (850 nm). In the $\nu_1 + 3\nu_3$ band some new lines have been observed [26]. One of them is shown in Fig. 9, where near a well know line a small absorption is present. This could be a rotational line splitting of the R21 by a local perturber via a Coriolis interaction [27]. In Fig. 10 is shown what has been observed not far from there by using the DA spectroscopy technique. Here the sloping backgroud is evident, showing the intrinsic operational characteristic of the DLs. Averaged results on self-broadening and shifting for some $\nu_1 + 3\nu_3$ lines are listed in Table 3.

In the same band situates the work of Dutta and colleagues [28] where the measured self-broadening coefficients are smaller than ours.

In the $2\nu_1 + \nu_2 + \nu_3$ we got the self-broadening FWHM coefficient only for the 11765.60 cm^{-1} (P7)

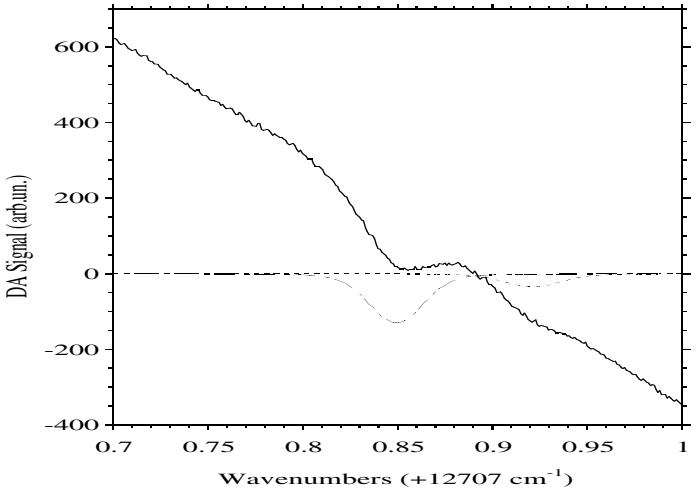

Figure 10: Acetylene absorption lines detected by DA at 42 Torr. The more intense of them is located at 12707.85 cm^{-1} ($\nu_1 + 3\nu_3$, R16). The other, whose origin is due probably to the same process than the one of Fig. 9, is at (12707.92 ± 0.01) cm^{-1}. The hatched lines are extracted by the fit.

Table 3: Averaged results of the observed acetylene FWHM self-broadening (γ_0) and shifting (S_0) coefficients in the $\nu_1 + 3\nu_3$ band.

$\gamma_0 = 11.6$ MHz/Torr	$S_0 = -0.7$ MHz/Torr

line:

$$\gamma_{0(\mathrm{P7})} = (13.2 \pm 0.6) \text{ MHz/Torr}$$

a value which is in the same range of the ones of the other band.

In the acetylene measurements we tested the goodness of the fit adopted when using the WM with 2^{nd} harmonic detection technique. Self-shifting coefficient measurements have been done by using either DA and WM techniques on the R21 line, the one of Fig. 9, and the results are plotted together in Fig. 11. In this figure the almost perfect parallelism of the best linear fits of the two sets of data shows that they have equal shift coefficients. The drift of the WM data to lower frequency is ought to a systematic phase difference between the two lock-in amplifiers used for the differential measurements and it is constant over all the pressure range.

In favorable conditions, that is at low pressure in a closed cell, and tuning the spectroscopic apparatus on the R15 line of the $\nu_1 + 3\nu_3$ band, some part per million per meter of path-length has been detected. In air at standard atmospheric pressure, where the monitoring can have important applications, 70 ppm

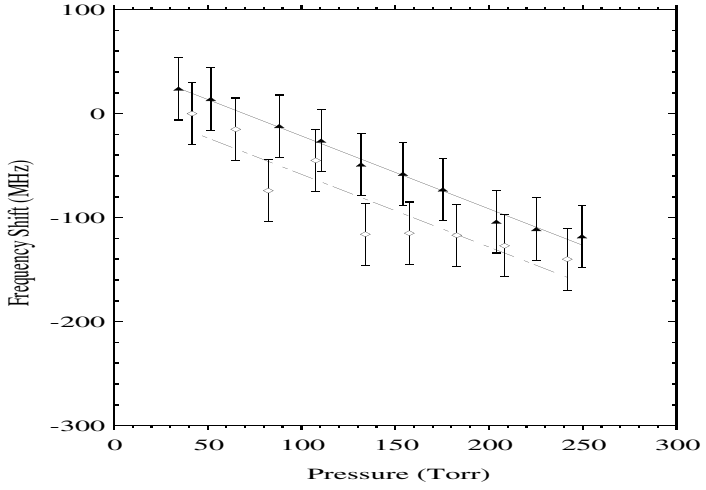

Figure 11: Frequency shift of the 12714.73 cm^{-1} absorption line as varying the acetylene pressure. The error in the pressure measurement was 5 Torr. The triangles refer to the DA measurements for which $S_{\mathrm{DA}} = (-0.7 \pm 0.2)$ MHz/Torr. The diamonds are related to the WM measurements [$S_{\mathrm{WM}} = (-0.7 \pm 0.3)$ MHz/Torr]. The best linear fits of the two sets of data are shown for comparison.

per meter of optical length have been revealed.

4.4 Methane

For detecting the methane overtone absorptions we used mostly the diode laser STC LT50A-03U, a single-mode multiple quantum well type, lasing at $\lambda \simeq 850$ nm at RT with a maximum output power of about 50 mW and an emission linewidth of a few MHz. Changing its temperature between -10 and 50°C, its emission wavelength ranged between 840 and 860 nm covering the $2\nu_1 + 2\nu_3$ band [1]. The Sharp LT024MD0 DL, whose emission is located around 780nm, has been used for tuning to the $3\nu_1 + \nu_3 + (\nu_2 \; or \; \nu_4)$ band. In fact its emission wavelength could span from 775 to 790 nm with a linewidth of some tens of MHz [26]. One example of methane absorption line detected by the WM spectrometer is shown in Fig. 12. The resonance is at 11574.48 cm^{-1} (863.737 nm @ 21°C) in the $2\nu_1 + 2\nu_3$ band; the methane gas pressure was 80 Torr giving a FWHM of 1.32 GHz, 80% Gaussian. Since some water vapor lines lie in the same spectral range, each observed resonance was identified as coming from methane or from water vapor by comparing the FM absorption signal with the one coming from another cell containing only water. Ought to its symmetry

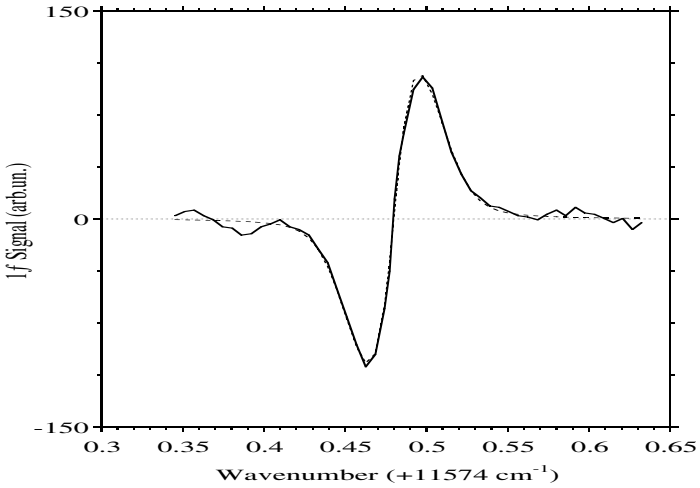

Figure 12: First derivative of the 11574.48 cm^{-1} methane absorption transition as observed at the lock-in output channel (τ = 12.5 ms) with the best fit (dashed line).

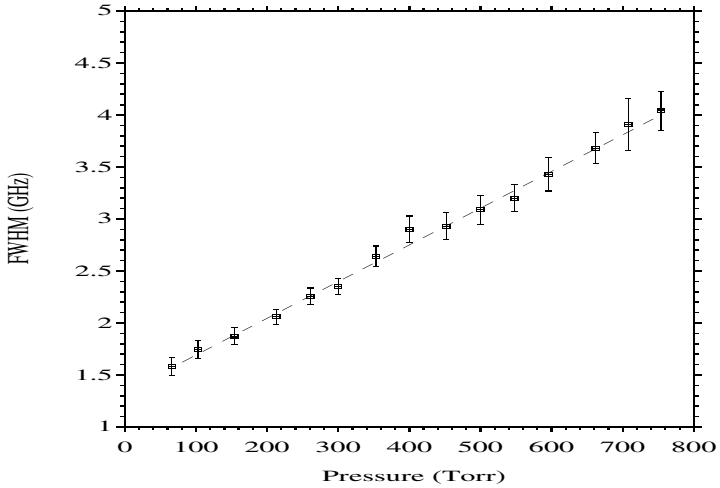

Figure 13: Absorption FWHM vs methane gas pressure for the 860.898 nm line, together with the best linear fit. The intercept is not zero because of the Doppler and the instrumental broadening.

Table 4: List of the observed *new* methane absorption lines.

Wavelength @ 21°C	Wavenumber
(nm)	(cm^{-1})
860.898	11612.66
860.928	11612.25
860.946	11612.01

(T_d) the methane molecule has no dipole momentum; it only creates a small dipole (δ_μ) along the C—H bind by the centrifugal force, lowering the symmetry to C_{3v}. For this reason its absorption lines, and particularly the overtones, are very weak and difficult to be detected.

With a path length of 5 meters and by using the WM spectroscopy technique on the 1^{st} harmonic ($1f$), we could follow the absorption line broadening process for some resonances, the more intense ones. Unfortunately in this case the S/N ratio was not enough to measure the line-shifting. Some observed lines are not yet classified; in fact in this region the band attribution is quite difficult because of the many possible overtone combinations [29]. We accurately measured the position of three of them within 0.01 cm^{-1}. They are listed in Table 4. Their intensities are comparable to the other methane absorption transitions reported in literature.

In Fig. 13 the 860.898 nm line the total FWHM is plotted as a function of the methane pressure. The higher is the pressure the higher is the error, because the derivative method worsens its performance as the line broadens. The linear fit of the experimental points gives the self-broadening coefficient (γ_0):

$$\gamma_0 = (3.5 \pm 0.2) \text{ MHz/Torr}.$$

By varying the pressure of N_2 and He buffer gases we obtained for the same line:

$$\gamma_{N_2} = (3.3 \pm 0.3) \text{ MHz/Torr},$$

$$\gamma_{He} = (1.5 \pm 0.2) \text{ MHz/Torr}.$$

The γ values obtained by Vujkovic Cvijin [30] and by Keffer [31] for the 619.68 nm overtone absorption line are similar to ours.

For many practical applications, methane at atmospheric pressure needs to be monitored in *open-path* configurations, where one has to deal with much broadened and overlapping lines together with external perturbations such as thermal flows, other gaseous species, etc.. The result is a much lower sensitivity than for low pressure conditions. In the present case, working in air, we could detect a CH_4 partial pressure corresponding to $\sim$ 5% of the total in a 5 m path. Obviously, by using a much longer path-length obtainable in a multipass cell, like the Herriott type one [32] we just acquired, the sensitivity could be increased at least ten times, to become competitive with the less selective but cheaper solid state based sensors.

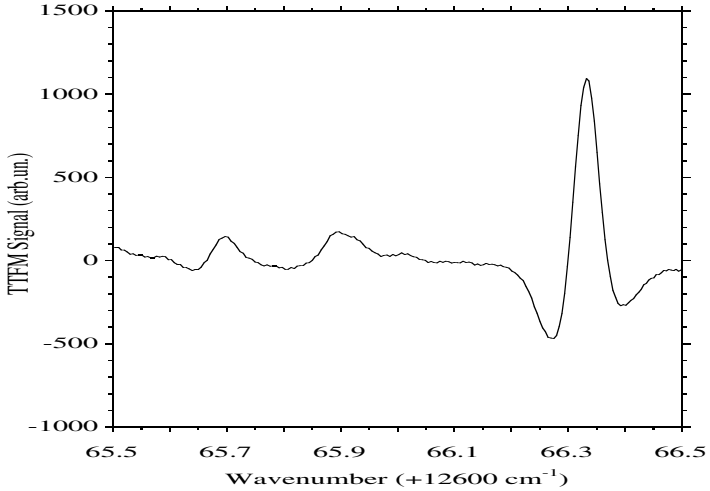

Figure 14: TTFM spectroscopy beat signal obtained for ammonia at $p = 35$ Torr, $T = 25°$C, 1 m absorption path, 100 Hz bandwidth. For the strongest line S/N is 60.

4.5 Ammonia

Ammonia has a relatively intense ro-vibrational absorption band in the 790 nm region, where the overtone $4\nu_1$ (symmetrical stretching) or the combination of overtones $2\nu_1 + 2\nu_3$ [33] (symmetrical and antisymmetrical stretchings) lie. More than fifty years ago spectroscopists [34] measured and tried a classification of the lines, but their spectral resolution was limited by diffraction and by the instrumentation available at that age. They used very long paths to overcome the problems related to the weakness of those lines. Now by using diode laser radiation with a good spectral resolution it is possible to better their results even with an optical path of few meters.
We used all the three techniques previously described depending on the strength of the absorption lines and the type of measurements to perform.

The Hitachi HL7806G DL emits at about 788 nm at RT, therefore by varying its temperature 20°C around RT it has been possible to range almost 8 nm and to embrace all the band located at 791.9 nm [4]. Taking advantage of the high resolving power and excellent S/N of the diode laser spectroscopic system, particularly the TTFMS one, we observed more absorption lines than those listed in literature. The wavenumbers of two of them have been accurately measured taking as reference a closest known line. Presumably they belong to one of the two bands $4\nu_1$ and $2\nu_1+2\nu_3$. As shown in Fig. 14, their intensities are lower than the neighboring 12666.32 cm^{-1} line ($\lambda = 789.285$ nm @ 25°C), for which the absorption coefficient at p = 35 Torr through a path $l = 1$ m has been measured to be $\alpha = 7 \times 10^{-5}$ cm^{-1}. In Table 5 wavelengths and wavenumbers of these *new* lines are listed.

Table 5: List of the observed *new* ammonia absorptions. For them $\alpha \approx 10^{-6}$ cm^{-1}.

Wavelength @ 25°C (nm)	Wavenumber (cm^{-1})
789.325	12665.69
789.312	12665.89

Table 6: Averaged results of the observed ammonia FWHM broadening (γ) and shifting (S) coefficients.

$\gamma_0 = 31.7$ MHz/Torr	$S_0 = 0.7$ MHz/Torr
$\gamma_{\text{air}} = 8.0$ MHz/Torr	$S_{\text{air}} = -0.5$ MHz/Torr
$\gamma_{\text{H}_2} = 8.7$ MHz/Torr	$S_{\text{H}_2} = -0.5$ MHz/Torr
$\gamma_{\text{He}} = 3.7$ MHz/Torr	$S_{\text{He}} = 0.0$ MHz/Torr

As usual on the more intense absorptions, pressure broadening coefficients have been measured at RT by using the WM or the DA techniques [35]. The average of the results for self-, air-, H_2-, He-broadening and shifting are listed in Table 6. Care has been used to control the ammonia adsorption from the measurement cells. In fact, as one of the authors observed [36], ammonia can stick to the walls of the cell and then induce a wrong partial pressure measurement when introducing the buffer gas. This phenomenon can be identified from a non linear behavior of the FWHM when varying the host gas pressure, particularly at low pressure. By choosing the right material or the appropriate internal coating of the cells, the problem can be reduced to acceptable limits.

There are not other measurements on this same band so far. On the fundamentals and in particular on the ν_2 and the ν_4, take place the works of Baldacchini and colleagues [37, 38] who measured and calculated self-broadening and shifting coefficients with values not far from ours. Measurements and calculations on pressure broadening of ammonia has been carried on also by Dhib and coworkers [39] still on the ν_4 band. With helium as host gas their results are little higher than ours.

An estimate of the spectrometer sensitivity has been done on the strong line of Fig. 14: by using the TTFM configuration we could still observe this

resonance in the measurement cell at 0.07 Torr in 1 m. In our experimental condition this means the detection of 6.4×10^{-8} g/cm^3 of ammonia per meter. In air at atmospheric pressure, the technique enabled to detect 50 ppm of NH_3 per meter with 1 Hz bandwidth.

5 Conclusions

FM overtone absorption spectroscopy of oxygen, water vapor, acetylene, methane and ammonia has been performed by using diode laser as sources, operating between 780 and 860 nm. New ro-vibrational overtone lines have been observed and measured for ammonia and acetylene in the 790 nm range. Pressure-broadening and shifting coefficients have been obtained by the aid of appropriate fits of the collected absorption features. The detection sensitivity has been evaluated in different measurement conditions. The technique shows enough sensitivity and resolving power to compete with the standard absorption spectroscopic methods that use more expensive devices. Detection of oxygen, water vapor, ammonia and acetylene as low as 50–70 ppm per meter of path has been reached at low pressure in a closed cell. Since all the system can be contained in a volume of a few dm^3, it is of real interest where a compactness of the device is required, as for instance in pollution control mobile stations or in aerospace vessels.
The excellent resolving power of the spectroscopic apparatus potentially permits to discriminate different gases in a complex atmosphere, with response times of a few hundreds of milliseconds. If needed, the resolving power can be increased at least by two orders of magnitude by adopting the *extended cavity* configuration with appropriate gratings.

Acknowledgements We wish to thank Dr. I. Longo for his precious guide and comments, and Mr. M. Tagliaferri, Mr. M. Badalassi, Mr. A. Barbini, Mr. R. Ripoli, whose technical support permitted this all.

References

[1] Vedder H. & Mecke R. 1933, Z. Phys. 86, 137.

[2] Baumann W. & Mecke R. 1933, Z. Phys. 81, 445.

[3] Hedfeld K. & Mecke R. 1932, Z. Phys. 77, 446.

[4] Badger R.M. & Mecke R. 1929, Z. Phys. Chem. 5, 333.

[5] Babcock H.D. & Herzberg L. 1948, Astrophys. J. 108, 167.

[6] Bjorklund G.C. 1980, Opt. Lett. 5, 15.

[7] Bjorklund G.C., Levenson M.D., Lenth W., Ortiz C. 1983, Appl. Phys. B32, 145.

[8] Pavone F.S., Marin F., Inguscio M., Ernst K. & Di Lonardo G. 1996, Appl. Opt. 32, 259.

[9] Wang L.G., Riris H., Carlisle C.B., Gallagher T.F. 1988, Appl. Opt. 27, 2071.

[10] Petermann K. 1991, Laser Diode Modulation and Noise, Kluwer Academic Publishers, The Netherlands.

[11] Edlén K. 1966, Metrologia 2, 71.

[12] Rothman L.S., Rinsland C.P., Goldman A., Massie S.T., Edwards D.P., Flaud J.-M., Perrin A., Camy-Peyret C., Dana V., Mandin J.-Y., Schroeder J., McCann A., Gamache R.R., Wattson R.B., Yoshino K., Chance K.V., Jucks K.W., Brown L.R., Nemtchinov V., Varanasi P. 1998, J. Quant. Spectrosc. Radiat. Transfer 60, 665.

[13] Lucchesini A., De Rosa M., Gabbanini C., Gozzini S., 1998, Nuovo Cimento D16, 117.

[14] De Rosa M., Ciucci A., Pelliccia D., Gabbanini C., Gozzini, S. Lucchesini A. 1998, Opt. Commun. 147, 55.

[15] D'Amato F. & Ciucci A. 1994, ENEA Report RT/INN/94/01.

[16] Phillips A.J., Hamilton P.A. 1995, J. Mol. Spectrosc. 174, 587.

[17] Ritter K.J. & Wilkerson T.D. 1987, J. Mol. Spectrosc. 121, 1.

[18] Ray B., Ghosh P.N. 1997, Spectrochim. Acta A53, 537.

[19] Ray B., Biswas D., Ghosh P.N. 1997, J. Mol. Struct. 407, 39.

[20] Brown L.R. & Plymate C. 2000, J. Mol. Spectrosc. 199, 166.

[21] Yang S., Canagaratna M.R., Witonsky S.K., Coy S.L., Steinfeld J.I., Field R.W. & Kachanov A.A. 2000, J. Mol. Spectrosc. 201, 188.

[22] Corsi C., Gabrysch M., Inguscio M. 1996, Opt. Commun. 128, 35.

[23] Cervelli F., Fuso F., Allegrini M. & Arimondo E. 1998, Appl. Surf. Sci. 127, 679.

[24] Grossmann B.E. & Browell E.V. 1989, J. Mol. Spectrosc. 136, 264.

[25] Lucchesini A., Gozzini S. & Gabbanini C. 2000, Eur. Phys. J. D8, 223.

[26] Lucchesini A., De Rosa M., Ciucci A., Gabbanini C., Gozzini S. 1996, Appl. Phys. B63, 277.

[27] Smith B.C. & Winn J.S. 1991, J. Chem. Phys. 94, 4120.

[28] Dutta B.K., Biswas D., Ray B. & Ghosh P.N. 2000, Eur. Phys. J. D11, 99.

[29] Dick K.A. & Fink U. 1977, J. Quant. Spectros. Radiat. Transfer 18, 433.

[30] Vujkovic Cvijin P., O'Brien J.J, Atkinson G.H., Wells W.K., Lunine J.I. & Hunten D.M. 1989, Chem. Phys. Lett. 159, 331.

[31] Keffer C.E., Conner C.P. & Smith W.H. 1986, J. Quant. Spectros. Radiat. Transfer 35, 495.

[32] Herriott D.R., Kogelnik H. & Kompfner R. 1964, Appl. Opt. 3, 523.

[33] Herzberg G. 1945, Infrared and Raman Spectra of Polyatomic Molecules, D. Van Nostrand Reinhold Co., New York, 296.

[34] Chao S.H. 1936, Phys. Rev. 50, 27.

[35] Lucchesini A., Pelliccia D., Gabbanini C., Gozzini S., & Longo I. 1994, Nuovo Cimento D16, 117.

[36] Baldacchini G., Bellatreccia A., D'Amato F. 1993, ENEA Report RT/INN/93/07.

[37] Baldacchini G., Buffa G. & Tarrini O. 1991, Nuovo Cimento D13, 719.

[38] Baldacchini G., Buffa G., D'Amato F., Tarrini O., De Rosa M., Pelagalli F. 2000, J. Quant. Spectros. Radiat. Transfer 67, 365.

[39] Dhib M., Bouanich J.-P., Aroui H. & Broquier M. 2000, J. Mol. Spectrosc. 202, 83.